HHS Public Access

Author manuscript

Clin Radiol. Author manuscript; available in PMC 2018 February 01.

Published in final edited form as:

Clin Radiol. 2017 February ; 72(2): 150–158. doi:10.1016/j.crad.2016.10.021.

Contrast-enhanced MDCT in patients with pancreatic neuroendocrine tumours: correlation with histological findings and diagnostic performance in differentiation between tumour grades

E. Belousova[a,b,*], **G. Karmazanovsky**[a,b], **A. Kriger**[c], **D. Kalinin**[d], **L. Mannelli**[e], **A. Glotov**[d], **N. Karelskaya**[a], **O. Paklina**[d,f], and **A. Kaldarov**[c]

[a]Department of Radiology, A.V. Vishnevsky Institute of Surgery, Moscow, Russia

[b]Department of Radiology, Faculty of Postgraduate Professional Training of Physicians, I.M. Sechenov First Moscow State Medical University, Moscow, Russia

[c]Department of Abdominal Surgery, A.V. Vishnevsky Institute of Surgery, Moscow, Russia

[d]Department of Pathology, A.V. Vishnevsky Institute of Surgery, Moscow, Russia

[e]Department of Radiology, Memorial Sloan Kettering Cancer Center, New York, NY, USA

[f]Department of Pathology, S.P. Botkin City Clinical Hospital, Moscow, Russia

Abstract

AIM—To identify the multidetector computed tomography (MDCT) features of pancreatic neuroendocrine tumours (pNETs), which correlate with tumour histology and enable preoperative grading.

MATERIALS AND METHODS—Thirty-nine patients with histologically confirmed pNET who underwent preoperative contrast-enhanced MDCT were included in this study. Nineteen tumours were classified as Grade 1 (G1) and 20 as Grade 2 (G2). Histopathology slides were reviewed to assess the intratumoural microvascular density (MVD) and the amount of tumour stroma. Computed tomography (CT) image analysis included tumour size, margin delineation, calcifications, homogeneity, contrast enhancement (CE) pattern, tumour absolute and relative enhancement, presence of cystic changes, pancreatic duct dilatation, regional and distant metastases. The diagnostic ability to predict tumour grade was measured for each MDCT finding and their combinations.

RESULTS—The mean arterial enhancement ratio had a mean±standard deviation of 1.53±0.45 in G1 and 1.01±0.33 in G2 pNETs (p=0.0003) and correlated with intratumoural microvascular density (MVD; r=0.55, p=0.0002). Tissue stroma percentage did not correlate with imaging findings. Late CE of the tumour (the peak attenuation observed in the venous phase) was significantly associated with G2. Tumour size ≥20 mm, arterial enhancement ratio <1.1, and late CE showed 74.4%, 79.5%, and 74.4% accuracy, respectively, in diagnosing G2 tumours, while the

[*]Guarantor and correspondent: E. Belousova, Department of Radiology, A.V. Vishnevsky Institute of Surgery, 27, Bolshaya Serpukhovskaya str., Moscow, 117997, Russia. Tel.: +7 985 927 70 49. dr.elena.belousova@gmail.com (E. Belousova).

accuracy of at least two of these criteria used in combination was 82%. Based on these results, a diagnostic algorithm was proposed, which showed high interobserver agreement (k=0.82) in the prediction of tumour grade.

CONCLUSION—Contrast-enhanced MDCT features correlate with histological findings and enable the differentiation between G1 and G2 pNETs during preoperative examination.

Introduction

Pancreatic neuroendocrine tumours (pNETs) are rare neoplasms that arise from the neuroendocrine cells of the pancreas. They represent <3% of all pancreatic malignancies, with an annual incidence of two cases per 100,000 persons per year.[1,2] Clinically, pNETs are classified as being functioning and non-functioning, based on their ability to produce a distinct clinical syndrome as a result of hormone hypersecretion. Among functioning tumours, insulinomas and gastrinomas are the most common types.[3] Nonfunctioning tumours are usually clinically silent and are discovered incidentally, unless they reach a size that causes compression or invasion of adjacent organs and become symptomatic. Incidental detection of pNETs during imaging procedures is increasing, raising questions regarding follow-up and treatment strategies.[4]

According to the recent World Health Organization 2010 classification, pNETs are classified based on their proliferative activity, evaluated by mitotic count or by Ki-67 index.[5] They are divided into three tumour grades: Grade 1 (G1) and 2 (G2) tumours, which are well-differentiated neuroendocrine tumours, and Grade 3 (G3) tumours, which are poorly differentiated neuroendocrine carcinomas. The new classification underlines the concept that all pNETs have a malignant potential. Tumour grade correlates significantly with prognosis and is an independent predictor of longterm survival.[6] The new classification, however, does not represent the tumour extent, for this purpose TNM (tumour–nodes–metastasis) staging is used.[7]

Somatostatin analogues or ablation may benefit patients with unresectable or residual disease, yet surgery remains the treatment of choice for any localized pNET, as it is associated with a significantly higher survival rate.[8] The treatment options include typical and atypical resections, such as tumour enucleation. Typical resections are associated with a high incidence of postoperative complications, as well as exo- and endocrine insufficiency.[9] Tumour enucleation, on the other hand, rarely results in exo- and endocrine impairment, and should be proposed for benign and borderline pancreatic neoplasms.[10] Tumour biopsy cannot provide sufficient information about tumour grade, due to the high heterogeneity of proliferative rates within a tumour.[11] In cases of tumour radio-frequency ablation, tumour grade cannot be assessed by histological examination.[12] As the risk of the presence of high-grade tumours cannot be completely excluded, there is a need for other strategies to enable pNETs to be graded preoperatively.

Imaging plays a crucial role in the diagnosis of pNETs, including tumour localization, differential diagnosis, and identification of signs of malignancy. Typically, pNETs are visualized as small, solid, hypervascular lesions in the arterial phase at computed tomography (CT).[13] As they include a heterogeneous group of tumours with different

histological grades, they may also present with non-specific findings, including the presence of calcifications, cystic or necrotic changes, and atypical patterns on contrast-enhanced images. Recent studies have focused on the assessment of imaging markers for the prediction of pNET aggressiveness, including tumour conspicuity in contrast-enhanced CT images, CT perfusion parameters, apparent diffusion coefficient (ADC) values on magnetic resonance imaging (MRI) images, and radionuclide uptake on positron-emission tomography (PET).[14–16] In the present study, the post-contrast CT images of pNETs were reviewed retrospectively with the aim of evaluating whether imaging features at CT can be used to differentiate between tumour grades. Additional histological examinations (the quantification of intratumoural microvessels and stroma) were also performed to explain the findings at CT. A diagnostic algorithm is proposed for the preoperative prediction of tumour grade.

Materials and methods

Patients

This retrospective study was reviewed and approved by the local ethics committee. Written informed consent was obtained from all patients. The institutional database was reviewed to select all patients who underwent surgical resection of pNETs between 2010 and 2016. Patients who underwent preoperative multiphase abdominal multi-detector (MD)CT within at least 60 days prior to surgery and with histological specimens available for a review were included in the study. Patients with tumours that were not visualized on preoperative CT (n=2) were excluded. Finally, the study population comprised 39 consecutive patients who met the inclusion criteria (17 men and 22 women, mean age 52±15.5 years). The overall number of tumours discovered was 44. Three patients had multiple sporadic tumours and one patient had multiple tumours as a part of multiple neuroendocrine neoplasia type 1 syndrome (MEN-1). When more than one tumour was observed, only the largest tumour was included in the analysis. Tumour lesions were located in the head (n=15), neck (n=4), body (n=7), and tail (n=13) of the pancreas.

CT imaging technique

CT was performed on one of two MD-row helical CT systems: Philips Brilliance CT-64 or Brilliance iCT-256 (Philips Healthcare, Cleveland, OH, USA) according to a standard protocol. The imaging parameters were as follows: 1–2 mm section thickness, beam pitch of 1, tube rotation speed of 0.75 seconds, 120 kVp tube voltage, automatic tube current modulation (150e500 mAs, Dose Right). Following the precontrast imaging, the high-concentrated contrast media, either iomeprol (400 mg iodine/ml) or iopamidol (370 mg iodine/ml; Bracco, Milan, Italy), was administered intravenously at a rate of 3–4 ml/s, using an autonomic dual-head pump injector. The bolus of contrast agent was followed by a saline chaser bolus (40–50 ml), injected at the same rate. The arterial, venous, and delayed-phase scans were obtained at 10, 35, and 180-second delays after aortic opacification had reached 100 HU.

Histopathological analysis

The tissue sections were stained with haematoxylin and eosin, and histopathological examination was performed in consensus by two pathologists. The diagnosis of pNET was confirmed using immunohistochemistry. According to the current WHO classification (2010), grading of pNETs was based on the Ki-67 index and mitotic rate per 10 high-power fields. The endothelial cell marker, CD-34, was used to identify tumour microvessels. Microvessel quantification was performed on the three microscopic fields at ×200 magnification (~1.8 mm^2) among the most vascularized areas ("hot spots"). Using the colour threshold instrument, the total number of pixels belonging to the vessels was determined, and this value was divided by the total number of pixels in the image. The presence of stromal tissue within the tumour was evaluated in all specimens stained with haematoxylin and eosin, and, depending on the percentage of stroma in the microscopic field (×100), was graded as follows: class I, having <25% stroma; class II, 25–50% stroma; and class III, >50% stroma.

Qualitative and quantitative image analysis

Two radiologists (with 2 and 7 years of experience) who were blinded to the tumour grade, evaluated the following CT features in consensus: tumour location, size, margin delineation, calcifications, homogeneity, presence of cystic changes, contrast enhancement (CE) pattern; presence of pancreatic duct dilatation, presence of regional and distant metastases. The tumour size was defined as the largest tumour diameter on axial scans. The tumour margins were defined as well-delineated (tumour margin smooth and clearly visible) or ill-delineated (with spiculation or infiltration on >90° of tumour perimeter). The presence of calcification within the tumour was recorded on unenhanced phase CT. Cystic changes within the tumour were defined as non-enhancing areas of circular or ovoid shape and well-defined margins. Pancreatic duct dilatation was defined as a duct diameter of ≥3 mm diameter.

The tumour attenuation (HU) was measured by placing an oval region of interest (ROI) of 10 mm^2, within the tumour on each phase of the image sets. Calcification, areas of cystic or necrotic change, vessels, and the pancreatic duct were carefully avoided. In cases of heterogeneity within the tumour, measurements were taken on the area that represented the predominant (>50%) tumour enhancement pattern. The relative tumour enhancement ratio was defined as the attenuation of the tumour divided by the attenuation of the normal pancreatic parenchyma, as measured on the arterial and portal venous phases, respectively. Tumours were also divided into those showing early CE and fast wash-out, with peak attenuation observed in the arterial phase (type A), and those showing late CE, with peak attenuation observed in the venous phase (type B). The tumour was considered to show wash-out if the attenuation in the venous phase was at least 10 HU lower than in the arterial phase.

Based on preliminary study results, a diagnostic algorithm to differentiate G2 tumours was proposed. Another two radiologists, with 3 and 9 years of experience in abdominal radiology, who were not involved with the previous work and were blinded to the grade, applied this algorithm to the same group of patients. They evaluated the tumour size, tumour enhancement ratio in arterial phase, and CE pattern retrospectively. Based on these findings,

they suggested a tumour grade for each pNET. Discrepancies between the two radiologists were resolved in consensus.

Statistical analysis

Descriptive statistics (mean, standard deviation, proportions) were calculated for all numerical data. The tumour-to-pancreas CE value was compared between tumour grades using the Mann–Whitney *U*-test. Arterial enhancement ratios for each tumour were compared with MVD using the Spearman correlation coefficient. MDCT features were compared between tumour grades and other histopathological findings using the chi-square and Fisher's exact test. A *p*-value <0.05 was considered to indicate a statistical significance for all analyses. The receiver operating characteristic (ROC) curves were drawn to determine the optimal quantitative cut-off values for the most significant ($p<0.001$) MDCT finding that could be used to differentiate between G1 and G2 pNETs. The sensitivity and specificity for differentiation between tumour grades was measured for each parameter and their combinations. The diagnostic ability of a proposed algorithm was evaluated using the chi-square test. To assess the interobserver agreement, Cohen's kappa analysis was performed; a κ index >0.8 was considered to be indicative of very good agreement. All statistical analyses were performed using Statistica, version 10.0 software package (StatSoft, Tulsa, OK, USA).

Results

At histopathology, 19 tumours were confirmed to be G1 pNETs and 20 tumours were G2 pNETs. The MVD ranged from 2% to 14.9% and correlated with tumour grade, being significantly higher in low-grade tumours: 7.8±2.5% (mean ±standard deviation) in G1 pNET versus 5.6±3.3% in G2 pNET, $p=0.0002$). The majority (35/39, 89.7%) of tumours had a minimal amount of stromal tissue (class I). The presence of excessive stromal tissue was detected in one G1 tumour (class II tumour), and in three G2 tumours (two class II and one class III tumours). The percentage of stromal tissue did not correlate significantly with tumour grade ($p=0.12$).

The data regarding MDCT features of pNETs in correlation with tumour grade are summarized in Table 1. Mean lesion size was significantly larger in G2 than in G1 tumours ($p=0.002$). There was no significant difference between the tumour grades with respect to the presence of pancreatic duct dilatation, tumour homogeneity, and the presence of calcification or cystic areas within the tumour. Liver metastases were observed in three patients, all of them with G2 tumours.

The mean attenuation of pNETs in the arterial phase was significantly higher in G1 tumours ($p=0.004$), while the difference in attenuation in the venous phase did not show statistical significance. The mean tumour-to-pancreas CE ratio in the arterial phase was more significant ($p=0.0003$; Fig 1). In the venous phase, the difference in relative the tumour-to-pancreas CE ratio also showed statistical significance ($p=0.01$). No statistically significant difference between tumour grades was observed with respect to the CE value in the delayed phase. The relative tumour-to-pancreas CE ratio had a strong correlation with intratumoural MVD according to histological examination ($r=0.55$, $p=0.0005$; Fig 2).

When reviewing the lesions according to their CE pattern, the majority of G1 tumours showed rapid wash-out in the venous phase: type A CE pattern (17/21, 80.9%), and the majority of G2 tumours showed slow wash-in and slow wash-out, with the peak CE observed in the venous phase: type B CE pattern (17/24, 70%; p=0.001). Examples of tumours with different grades are represented in Figs 3 and 4.

ROC curves were obtained to find the most statistically significant MDCT finding to obtain the optimal cut-off values. The area under curve was 0.86 for the arterial enhancement ratio, 0.80 for the CE pattern, and 0.76 for tumour size. Tumour size >2 cm, arterial enhancement ratio <1.1 and type B enhancement pattern was used as the cut-off values to determine the sensitivity and specificity of prediction of G2 pNETs. Table 2 represents the MDCT features in correlation with the histopathological findings that affect patient prognosis and survival after surgery. Importantly, only lesions with an arterial enhancement ratio of <1.1, type B CE pattern, and size >2 cm had liver metastases. Commonly, size <2 cm is used as a prognostic indicator for G1 tumours, but in the present study seven lesions with size <2 cm were further confirmed to be G2 tumours. Among these tumours, four had an arterial CE ratio <1.1 and a type B CE pattern.

The sensitivity, specificity, positive predictive value (PPV), negative predictive value (NPV), and accuracy for each MDCT finding and their combinations are represented in Table 3. The combination of all three findings showed the highest specificity, but the lowest sensitivity. The highest accuracy (82%) was shown by the combination of at least two out of the three findings. Based on these results, a diagnostic algorithm was proposed for determining G2 pNETs (Fig 5). Two radiologists independently reviewed the CT images using the algorithm: tumours of <2 cm and an arterial enhancement ratio of >1.1 were classified as G1 pNETs, and tumours of >2 cm and with an arterial enhancement ratio of <1.1 were classified as G2 pNETs. In cases of discrepancy, another parameter, type of CE pattern, was used to determine the tumour grade. The two reviewers showed very good interobserver agreement (k=0.82), and there were only three cases of disagreement. They predicted the tumour grade with 76.9% accuracy (p=0.001).

Discussion

It is generally accepted (in breast tumours, lung tumours, etc.) that rich angiogenesis, which is assessed by calculating the MVD, can be predictive of a poor outcome.[17] In contrast, the relationship between vascularization degree and aggressiveness in neuroendocrine tumours is the opposite. pNETs are usually hypervascular, as they arise from pancreatic islet cells, which themselves have rich vascularization, and the tissue microarchitecture is preserved in low-grade tumours. With progression to malignancy, tumour vascularization is modified, resulting in an abnormal CE pattern: either hypovascularity in the arterial phase or late CE in the venous phase.[18,19] This is in contrast to what is seen in, for example, pancreatic adenocarcinomas, where high MVD is associated with decreased survival.[20]

This conception is proved by a number of previous studies. d'Assignies *et al.*[15] reported of a high correlation between MVD and tumour grade, and that tumour blood flow, assessed by perfusion CT, correlated with intratumoural MVD and was significantly higher in the

tumours with a Ki-67 proliferation index of ≤2%. Relative tumour enhancement on the arterial phase CT images showed good correlation with MVD and tumour grade in the present study (p=0.0005 and p=0.0003, respectively); however, MVD is usually counted in "hot spot" areas (the areas of highest vascularization) while the ROI used to measure the HU density, captures a larger area of both high and low vascularization. Thus, despite the good correlation with histological findings, the relative CE ratio of the tumour alone cannot be used to predict the tumour grade.

Few studies have focused on the additional CE characteristics that are useful for the assessment of pNET grade. Among them, Cappelli *et al.*[21] showed that some pNETs have a progradient CE, becoming more conspicuous in the delayed phase, which was proven to be a pathognomonic sign for well-differentiated neuroendocrine carcinomas. Conversely, all tumours showing early CE and fast wash-out were well-differentiated tumours with benign and uncertain behaviour, according to the 2004 WHO classification system. The present study also showed a high correlation between tumour CE pattern and grade: 89% of type A lesions were graded as G1 and 70% of type B lesions were graded as G2 (p=0.001).

Although the present results showed a significant correlation between the intratumoural MVD and arterial enhancement ratio, the correlation was not significant between intratumoural MVD and CE type (p=0.07). Indeed, the MVD percentage explains the amount of contrast media administered to the tumour tissue, but not the timing of enhancement. CE type (early or late) reflects the balance between the blood supply and retention of contrast agent in the interstitial spaces.[22] This phenomenon could be attributed to the desmoplastic response in pNETs, similar to that seen in cholangiocarcinoma, where extensive fibrosis obstructs the clearance of the contrast media, leading to a continuous increase in CE.[23] Therefore, the amount of stromal tissue in each pNET was evaluated. Three out of four (75%) tumours with well-developed stroma were graded as G2 pNETs, yet the difference between CE type and the percentage of stroma was not statistically significant. The present results are different from those reported by Tatsumoto *et al.*,[11] where the difference in the amount of stromal tissue between different enhancement patterns reached statistical significance. This discrepancy can be attributed to the lack of G3 tumours in the present study.[11,21]

Previous studies have proven that tumour size >2 cm is predictive of malignancy.[24] According to the present findings, G1 tumours were significantly smaller than G2 tumours (p=0.002). Tumour size is also an important factor in determining the T-stage of pNETs: tumours of 2–4 cm are classified as T2 stage.[25] In the present study, seven out of 20 G2 tumours were <2 cm, and these tumours could have been wrongly classified as G1 if relying on their size alone. As a result of the high rate of atypical post-contrast behaviour in G2 pNETs, a more aggressive behaviour could be predicted during preoperative staging, even in small tumours.[26,27]

As for other atypical imaging findings in pNETs, such as tumour heterogeneity, pancreatic duct dilatation, and the presence of liver metastases, data in the literature vary. Luo *et al.*[28] reported significant differences among tumours of different grades regarding tumour margin delineation, dilatation of the pancreatic duct, and the presence of distant metastases.

Poultsides *et al.*[29] reported that calcified tumours were larger and more commonly associated with the presence of metastasis and intermediate tumour grade.[29] The present results are similar to those of Takumi *et al.*,[26] where no significant differences were observed between G1 and G2 pNETs with respect to tumour delineation, pancreatic duct dilatation, or the presence of calcification. The reason for such a discrepancy between the different results can be attributed to the lack of G3 pNETs in the present study and that of Takumi *et al.* Nonetheless, it is important to note that all pNETs with liver metastasis had atypical MDCT findings in the present study.

Predominantly cystic neuroendocrine tumours are less commonly associated with lymph node and liver metastases and have a higher recurrence-free survival rate as compared to solid tumours, but due to large cystic areas, they can reach a size suggestive of tumour malignancy.[30,31] Thus, additional imaging markers are important in the preoperative grading of cystic pNETs; however, the number of pNETs with cystic transformation was relatively small in the present study, and the presence of cystic change did not correlate significantly with tumour grade.

In the present study, both the tumour arterial enhancement ratio and enhancement pattern were found to be comparable to tumour size regarding the prediction of tumour grade (74.4% and 79.5% versus 74.4% accuracy, respectively). In addition, a combination of at least two out of the three CT features, tumour size >2cm, arterial enhancement ratio <1.1 and type B CE pattern, led to an increase in diagnostic accuracy up to 82% in the differentiation of G2 from G1 pNETs. A diagnostic algorithm, provided by the present study, enables the preoperative prediction of G2 pNET with very good interobserver agreement. The authors recommend beginning with the evaluation of tumour size and the arterial enhancement ratio. In cases of discrepancy between these two results, another parameter, CE type, should be evaluated to confirm the diagnosis.

One limitation of the present study is the lack of neuroendocrine carcinomas: G3 pNETs. This can be explained by the fact that the CT–histopathology correlation is based on the examination of surgically resected material, and neuroendocrine carcinomas are rarely referred for surgery; however, low-grade neuroendocrine tumours usually have obvious landmarks of malignancy, e.g., necrotic change, presence of vascular invasion, and metastases.[27] A second limitation is that tumours that were not visible on preoperative CT were excluded, as the evaluation of their CT parameters was impossible.

In conclusion, tumour size >2cm, arterial enhancement ratio <1.1, and late CE are indicative of G2 pNETs. This information can be used to support decisions considering the extent of tumour resection or the possibility of a conservative approach, allowing for individualized decision making. Tumours <2 cm should be viewed with higher caution if they show atypical behaviour on contrast-enhanced CT.

References

1. Halfdanarson TR, Rabe KG, Rubin J, et al. Pancreatic neuroendocrine tumours (pNETs): incidence, prognosis and recent trend toward improved survival. Ann Oncol. 2008; 19:1727–33. [PubMed: 18515795]

2. Yao JC, Hassan M, Phan A, et al. One hundred years after ”carcinoid”: epidemiology of and prognostic factors for neuroendocrine tumours in 35,825 cases in the United States. J Clin Oncol. 2008; 26:3063–72. [PubMed: 18565894]

3. Jensen RT, Cadiot G, Brandi ML, et al. ENETS Consensus Guidelines for the management of patients with digestive neuroendocrine neoplasms: functional pancreatic endocrine tumour syndromes. Neuroendocrinology. 2012; 95(2):98–119. [PubMed: 22261919]

4. Rosenberg AM, Friedmann P, Del Rivero J, et al. Resection versus expectant management of small incidentally discovered nonfunctional pancreatic neuroendocrine tumours. Surgery. 2016; 159(1): 302–9. [PubMed: 26547726]

5. Klimstra, DS., Arnold, R., Capella, C. Neuroendocrine neoplasms of the pancreas. In: Bosman, FT.Carneiro, F.Hruban, RH., et al., editors. WHO classification of tumours of the digestive system. Lyon: IARC Press; 2010. p. 322-6.

6. Scarpa A, Mantovani W, Capelli P, et al. Pancreatic endocrine tumours: improved TNM staging and histopathological grading permit a clinically efficient prognostic stratification of patients. Mod Pathol. 2010; 23:824–33. [PubMed: 20305616]

7. Rindi G, Klöppel G, Alhman H, et al. TNM staging of foregut (neuro) endocrine tumours: a consensus proposal including a grading system. European Neuroendocrine Tumour Society (ENETS). Virchows Arch. 2006; 449(4):395–401. [PubMed: 16967267]

8. Hill JS, McPhee JT, McDade TP, et al. Pancreatic neuroendocrine tumours: the impact of surgical resection on survival. Cancer. 2009; 115:741–51. [PubMed: 19130464]

9. Smith JK, Ng SC, Hill JS, et al. Complications after pancreatectomy for neuroendocrine tumours: a national study. J Surg Res. 2010; 163:63–8. [PubMed: 20599224]

10. Hackert T, Hinz U, Fritz S, et al. Enucleation in pancreatic surgery: indications, technique, and outcome compared to standard pancreatic resections. Langenbecks Arch Surg. 2011; 396:1197–203. [PubMed: 21553230]

11. Tatsumoto S, Kodama Y, Sakurai Y, et al. Pancreatic neuroendocrine neoplasm: correlation between computed tomography enhancement patterns and prognostic factors of surgical and endoscopic ultrasound-guided fine-needle aspiration biopsy specimens. Abdom Imaging. 2013; 38(2):358–66. [PubMed: 22945422]

12. Rossi S, Viera FT, Ghittoni G, et al. Radiofrequency ablation of pancreatic neuroendocrine tumours: a pilot study of feasibility, efficacy, and safety. Pancreas. 2014; 43(6):938–45. [PubMed: 24717825]

13. McAuley G, Delaney H, Colville J, et al. Multimodality preoperative imaging of pancreatic insulinomas. Clin Radiol. 2005; 60(10):1039–50. [PubMed: 16179163]

14. Kim JH, Eun HW, Kim YJ, et al. Staging accuracy of MR for pancreatic neuroendocrine tumour and imaging findings according to the tumour grade. Abdom Imaging. 2013; 38(5):1106–14. [PubMed: 23728305]

15. d’Assignies G, Couvelard A, Bahrami S, et al. Pancreatic endocrine tumours: tumour blood flow assessed with perfusion CT reflects angiogenesis and correlates with prognostic factors. Radiology. 2009; 250(2):407–16. [PubMed: 19095784]

16. Durán HJ, Ielpo B, Díaz E, et al. Predictive prognostic value of local and distant recurrence of F-fluorodeoxyglucose positron emission tomography for pancreatic neuroendocrine tumours with reference to World Health Organization classifications (2004, 2010). Case series study. Int J Surg. 2016; 29:176–82. [PubMed: 27063856]

17. Bergers G, Benjamin LE. Tumour genesis and the angiogenic switch. Nat RevCancer. 2003; 3:401–10.

18. Marion-Audibert AM, Barel C, Gouysse G, et al. Low microvessel density is an unfavorable histoprognostic factor in pancreatic endocrine tumours. Gastroenterology. 2003; 125:1094–104. [PubMed: 14517793]

19. Takahashi Y, Akishima-Fukasawa Y, Kobayashi N, et al. Prognostic value of tumour architecture, tumour-associated vascular characteristics, and expression of angiogenic molecules in pancreatic endocrine tumours. Clin Cancer Res. 2007; 13(1):187–96. [PubMed: 17200354]

20. Hattori Y, Gabata T, Matsui O, et al. Enhancement patterns of pancreatic adenocarcinoma on conventional dynamic multidetector row CT: correlation with angiogenesis and fibrosis. World J Gastroenterol. 2009; 15(25):3114–21. [PubMed: 19575490]
21. Cappelli C, Boggi U, Mazzeo S, et al. Contrast enhancement pattern on multidetector CT predicts malignancy in pancreatic endocrine tumours. Eur Radiol. 2015; 25(3):751–9. [PubMed: 25447971]
22. Tang L, Li ZY, Li ZW, et al. Evaluating the response of gastric carcinomas to neoadjuvant chemotherapy using iodine concentration on spectral CT: a comparison with pathological regression. Clin Radiol. 2015; 70(11):1198–204. [PubMed: 26188843]
23. Asayama Y, Yoshimitsu K, Irie H, et al. Delayed-phase dynamic CT enhancement as a prognostic factor for mass-forming intrahepatic cholangiocarcinoma. Radiology. 2006; 238:150–5. [PubMed: 16304089]
24. Bettini R, Partelli S, Boninsegna L, et al. Tumour size correlates with malignancy in nonfunctioning pancreatic endocrine tumour. Surgery. 2011; 150(1):75–82. [PubMed: 21683859]
25. Bosman, FT. WHO Classification of Tumour of the Digestive System. Lyon: IARC Press; 2010.
26. Takumi K, Fukukura Y, Higashi M, et al. Pancreatic neuroendocrine tumours: correlation between the contrast-enhanced computed tomography features and the pathological tumour grade. Eur J Radiol. 2015; 84(8):1436–43. [PubMed: 26022520]
27. Kim JH, Eun HW, Kim YJ, et al. Pancreatic neuroendocrine tumour (PNET): staging accuracy of MDCT and its diagnostic performance for the differentiation of PNET with uncommon CT findings from pancreatic adenocarcinoma. Eur Radiol. 2016; 26(5):1338–47. [PubMed: 26253257]
28. Luo Y, Dong Z, Chen J, et al. Pancreatic neuroendocrine tumours: correlation between MSCT features and pathological classification. Eur Radiol. 2014; 24(11):2945–52. [PubMed: 25048189]
29. Poultsides GA, Huang LC, Chen Y, et al. Pancreatic neuroendocrine tumours: radiographic calcifications correlate with grade and metastasis. Ann Surg Oncol. 2012; 19(7):2295–303. [PubMed: 22396008]
30. Kawamoto S, Johnson PT, Shi C, et al. Pancreatic neuroendocrine tumour with cystlike changes: evaluation with MDCT. AJR Am J Roentgenol. 2013; 200(3):W283–90. [PubMed: 23436873]
31. Cloyd, JM., Kopecky, KE., Norton, JA., et al. Neuroendocrine tumours of the pancreas: degree of cystic component predicts prognosis. Surgery. 2016. http://dx.doi.org/10.1016/j.surg.2016.04.005. pii: S0039-6060(16) 30036–8

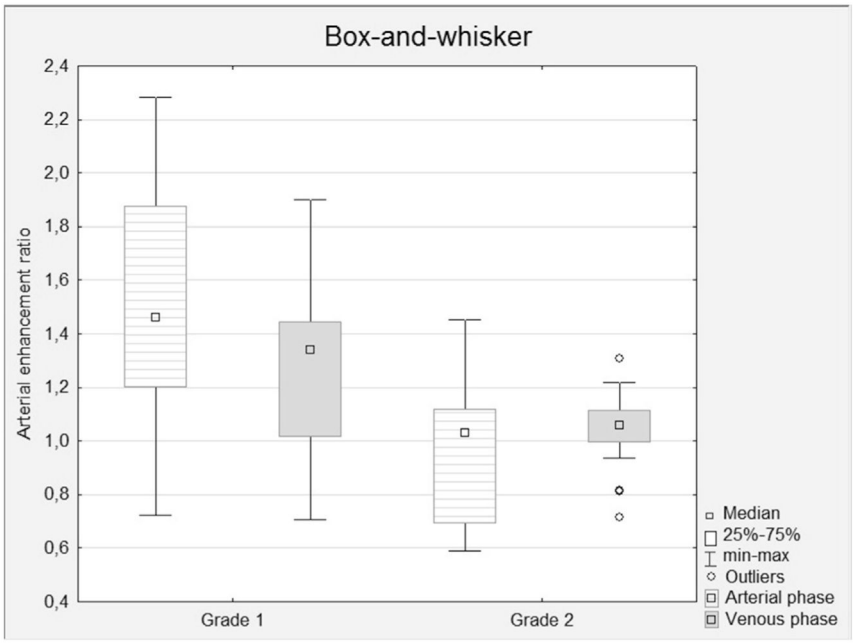

Figure 1.

Box-and-whisker plots of the relative enhancement ratios in G1 and G2 pNETs, evaluated in the arterial, venous, and delayed phases. The enhancement ratios show a statistical difference between grades in the arterial (p=0.0003) and venous (p=0.01) phases.

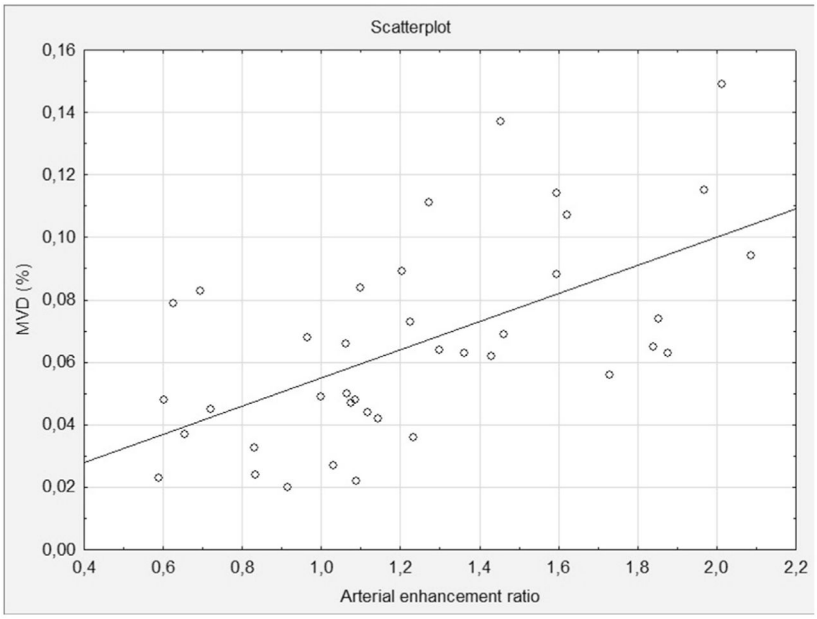

Figure 2.

The relative arterial enhancement ratio in correlation with intratumoural MVD (r=0.55, p=0.0005)

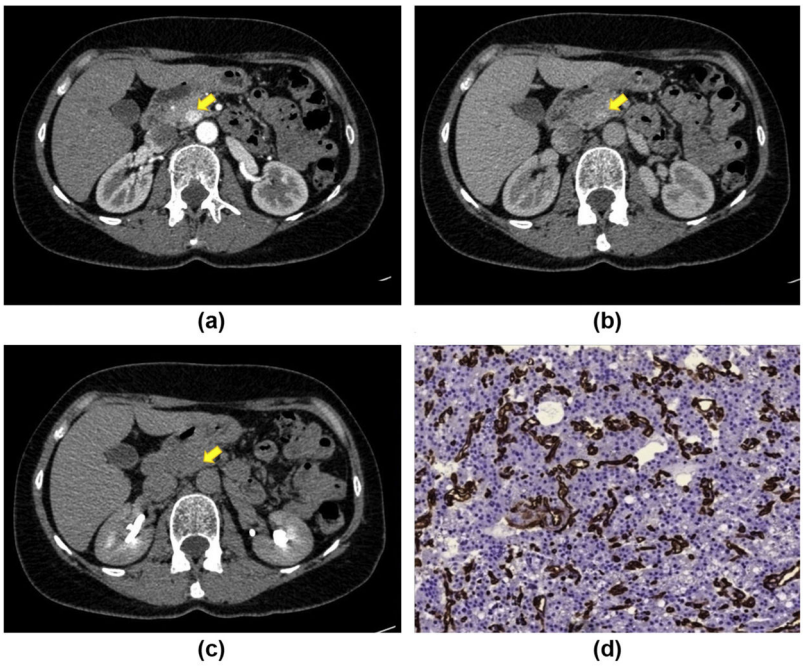

Figure 3.

CT post-contrast appearance of a G1 pNET: a small lesion in the pancreatic head (yellow arrow) shows early enhancement during the arterial phase (a) with wash-out in the venous (b) and delayed (c) phases (type A CE pattern). The lesion has an arterial enhancement ratio of >1.1. (d) Immunostaining with CD34 antibody (×200) highlights vessels (red), showing that the intratumoural MVD is high (14%)

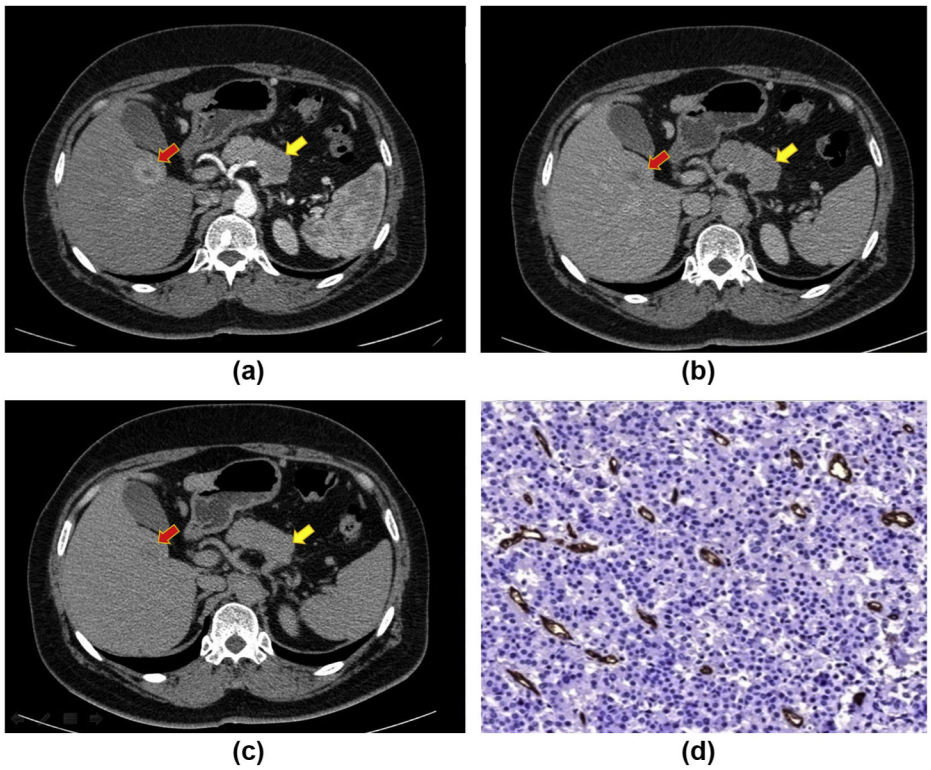

Figure 4.

CT post-contrast appearance of a G2 pNET: a lesion in the pancreatic body (yellow arrow) shows hypoattenuation in the arterial phase (a) and hyperattenuation in the venous (b) and delayed (c) phases (type B CE pattern). The lesion has an arterial enhancement ratio of <1.1. Note the metastatic lesion (red arrow) in the right liver lobe with peripheral rim enhancement. (d) Immunostaining with CD34 antibody highlights vessels (red), showing that the intratumoural MVD is low (4%).

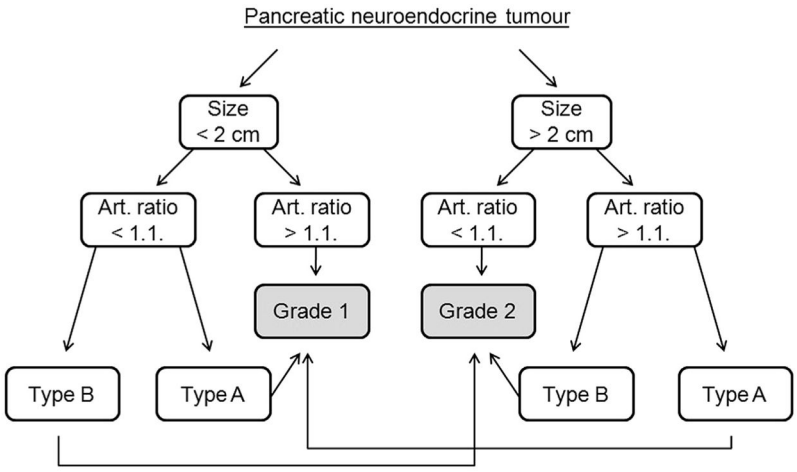

Figure 5.
The diagnostic algorithm for differentiation between G1 and G2 pNETs.

Table 1

Qualitative and quantitative computed tomography features of pancreatic neuroendocrine tumours according to the World Health Organization tumour classification.

Threshold criterion	Grade 1 (*n*=19)	Grade 2 (*n*=20)	*p*-Value
Mean tumour size	15.2±4.7	30.2±17.3	0.002
Tumour contrast enhancement			
Arterial phase	147±45	104.2±39.4	0.004
Venous phase	107.9±26.2	93.3±23	NS
Delayed phase	78.5±18.5	71.4±15.6	NS
Tumour-to-pancreas contrast ratio			
Arterial phase	1.53±0.45	1.01±0.33	0.0003
Venous phase	1.29±0.32	1.03±0.13	0.01
Delayed phase	1.14±0.27	1.06±0.13	NS
Contrast enhancement pattern			
Type A	17	6	0.001
Type B	2	14	
Homogeneity			
Homogeneous	16	13	NS
Non-homogeneous	3	7	
Tumour delineation			
Clear	18	15	NS
Non-clear	1	5	
Upstream pancreatic duct dilatation			
Present	1	2	NS
Absent	18	18	
Cystic or necrotic change			
Present	3	5	NS
Absent	16	15	
Calcifications			
Present	2	3	NS
Absent	17	17	
Liver metastases			
Present	0	3	NS
Absent	19	17	

NS, non-significant.

Table 2

Correlation of computed tomography features with the histopathological findings of pancreatic neuroendocrine tumours.

Histological data	Contrast enhancement pattern		p-Value	CE		p-Value	Size		p-Value
	Type A (*n*=23)	Type B (*n*=16)		<1.1 (*n*=18)	>1.1 (*n*=21)		<2 cm (*n*=23)	>2 cm (*n*=16)	
Tumour grade									
Grade 1 (*n*=19)	17	2	0.001	4	15	0.002	16	3	0.002
Grade 2 (*n*=20)	6	14		14	6		7	13	
Liver metastases									
present (*n*=3)	0	3	NS	3	0	NS	0	3	NS
absent (*n*=36)	23	13		15	21		23	13	
Lymph node metastases[a]									
present (*n*=7)	3	4	NS	5	2	0.02	1	6	0.001
absent (*n*=22)	21	9		15	15		22	8	

[a]Lymph nodes were assessed histologically in 29 patients.

Table 3

Diagnostic accuracy of multidetector computed tomography (MDCT) in determining the Grade 2 pancreatic neuroendocrine tumours.

MDCT criteria	Sensitivity	Specificity	PPV	NPV	Accuracy
Arterial enhancement ratio <1.1	70	78.9	77.8	71.4	74.4
Size >2 cm	65	84.2	81.3	69.6	74.4
Type B contrast enhancement	70	89.5	87.5	73.9	79.5
Combination of at least two out of three findings	75	89.4	88.2	77.2	82
Combination of three findings	45	94.7	90	62	69.2